T Cell Receptor Grafting allows Virological Control of Hepatitis B Virus Infection

Karin Wisskirchen[1,2,3,*,#], Janine Kah[3,4,#], Antje Malo[1], Theresa Asen[1], Tassilo Volz[4], Lena Allweiss[4], Jochen M. Wettengel[2], Marc Lütgehetmann[3,5], Stephan Urban[3,6], Tanja Bauer[1,2,3], Maura Dandri[3,4#], Ulrike Protzer[1,2,3,*,#]

[1]Institute of Virology, Helmholtz Zentrum München, Munich, Germany.

[2]Institute of Virology, School of Medicine, Technical University of Munich, Munich, Germany.

[3]German Centre for Infection Research (DZIF), Munich, Hamburg and Heidelberg partner sites, Germany.

[4]I. Department of Internal Medicine, University Medical Center Hamburg-Eppendorf, Hamburg, Germany.

[5]Institute of Microbiology, Virology and Hygiene, University Medical Center Hamburg-Eppendorf, Hamburg, Germany

[6]Department of Infectious Diseases, Molecular Virology, University Hospital Heidelberg, Heidelberg, Germany

[#]Equal contribution

*Corresponding authors

Prof. Ulrike Protzer, MD, Institute of Virology, Trogerstrasse 30, 81675 Munich, Germany, +49-89-4140-6886, protzer@tum.de, protzer@helmholtz-muenchen.de

Karin Wisskirchen, PhD, Institute of Virology, Trogerstrasse 30, 81675 Munich, Germany, +49-89-4140-6814, karin.wisskirchen@tum.de

Words: 9432

Ulrike Protzer, Karin Wisskirchen and Antje Malo hold shares of and serve as advisors for SCG Cell Therapy Pte. Ltd.. Stephan Urban holds patent rights on Myrcludex B. The other authors have declared that no conflict of interest exists.

Abstract

T cell therapy is a promising means to treat chronic HBV infection and HBV-associated hepatocellular carcinoma. T cells engineered to express an HBV-specific T cell receptor (TCR) may achieve cure of HBV infection upon adoptive transfer. We investigated the therapeutic potential and safety of T cells stably expressing high affinity HBV envelope- or core-specific TCRs recognizing European and Asian HLA-A2 subtypes. Both $CD8^+$ and $CD4^+$ T cells from healthy donors and from chronic hepatitis B patients became polyfunctional effector cells when grafted with HBV-specific TCRs and eliminated HBV from infected HepG2-NTCP cell cultures. A single transfer of TCR-grafted T cells into HBV-infected, humanized mice controlled HBV infection and virological markers declined 4-5 log or below detection limit. When – as in a typical clinical setting - only a minority of hepatocytes were infected, engineered T cells specifically cleared infected hepatocytes without damaging non-infected cells. Cell death was compensated by hepatocyte proliferation and alanine amino transferase levels peaking at day 5-7 normalized again thereafter. Co-treatment with the entry inhibitor Myrcludex B ensured long-term control of HBV infection. Thus, T cells stably transduced with highly functional TCRs have the potential to mediate clearance of HBV-infected cells causing limited liver injury.

Keywords: chronic hepatitis B; hepatocellular carcinoma; adoptive T-cell therapy; functional cure; humanized mice, Myrcludex B

Introduction

Worldwide, more than 250 million humans suffer from chronic hepatitis B (CHB), which accounts for an estimated 880.000 deaths per year caused by secondary complications like liver cirrhosis or hepatocellular carcinoma (HCC) (1). Current therapeutic regimens based on the use of nucleos(t)ide analogues (NUCs) can efficiently suppress viral replication, but are unable to eradicate the virus. The so-called covalently closed circular DNA (cccDNA) of HBV persists as a transcription template in the nucleus of infected cells and re-initiates HBV replication when antiviral treatment is discontinued (2). Hence, therapeutic options are needed, in which cccDNA is eliminated or at least strongly reduced and controlled by the immune system to allow functional HBV cure and to prevent relapse (3).

During acute, resolving hepatitis B a strong immune response is mounted with T cells being key to clear the virus (4). In CHB by contrast, the scarce and oligoclonal T-cell response against HBV fails to control the virus and to prevent disease progression (5). T cells have been shown to kill infected hepatocytes and to secrete cytokines that control virus replication in a non-cytolytic fashion by silencing (6-8) but also by destabilizing cccDNA (9, 10). In addition, killing of HBV-infected cells will promote compensatory cell proliferation that in turn favors further cccDNA loss by cell division (11).

Restoring a potent T-cell response by adoptive T-cell therapy is an interesting therapeutic option (12, 13). The concept of transferring adaptive immunity to control HBV has already been applied successfully in CHB patients who underwent stem cell transplantation and received bone marrow from HBV-immune donors (14-16). Since allogeneic stem cell transplantation is limited by its severe side effects like graft-versus-host disease and a high mortality, alternative approaches are required. Genetic engineering of autologous T cells to express HBV-specific receptors is an attractive alternative to treat CHB, to prevent HBV-related complications or to treat HBV-related HCC (17).

We have already demonstrated that T cells expressing a chimeric antigen receptor binding the antigenic loop within the "S"-domain of all HBV envelope proteins selectively eliminated HBV-infected and thus cccDNA-positive target cells (18, 19). It has also been shown that T cells from HBV-infected patients can be engrafted with T cell receptors (TCR) against the envelope or the core protein and become activated upon recognition of HBV peptides (20, 21). Moreover, significant reduction of HBV infection in humanized mice has recently been demonstrated after repeated adoptive transfers of human T cells engineered to express HBV-specific TCRs via mRNA electroporation (22). However, due to the transient expression of the TCR and the high numbers of infected cells present in that experimental setting, the antiviral effects remained limited and HBV rebound was observed within ten days after the last T cell injection. Most likely, a more sustained T cell activity, ideally combined with strategies aiming at blocking new infection events (23), is required to achieve a more profound and durable control of HBV infection. We recently reported the cloning, characterization and permanent expression of a set of eleven HBV-specific TCRs and determined their functional avidity (21). This allowed us to identify those most promising TCRs for adoptive T cell therapy.

In the present study, we aimed at determining the potential of T cells grafted by retroviral vector transduction with HBV-specific TCRs to clear HBV-infected cells without damaging non-infected neighboring cells. Furthermore, we combined T cell therapy with the virus entry inhibitor Myrcludex B (MyrB) (24) to restrict new virus spread after T-cell control of HBV infection, and showed that T cells grafted with selected, high avidity TCRs were able to control HBV-infection both in cultured hepatocytes and in vivo in livers of HBV-infected humanized mice.

Results

Core- and S-specific TCRs confer HBV-specificity upon retroviral transduction

HLA-A2 restricted HBV envelope- or core-specific TCRs were cloned as gene-optimized constructs into a retroviral vector. TCR-transgenic T cells were generated by retroviral transduction resulting in high expression of both TCRs on $CD4^+$ as well as $CD8^+$ T cells (Figure 1A). Functional avidities of eleven TCRs were compared in extensive analyses resulting in a functionality rating as described in detail in Wisskirchen et al. (21) (Supplemental table 1). The $core_{18\text{-}27}$ (C_{18})-specific TCR $6K_{C18}$ and the $S_{20\text{-}28}$ (S_{20})-specific TCR $4G_{S20}$ were selected for comprehensive testing of their antiviral activity. Transduced T cells killed stable HBV-replicating hepatoma cells in co-cultures at effector to target (E:T) ratios as low as 1:12. At an E:T ratio of 1:3, core-specific, $6K_{C18}$-grafted T cells eliminated 50% of HBV-replicating cells after 6-7 hours. S-specific, $4G_{S20}$-grafted T cells showed slower kinetics and needed about 20 hours (Figure 1B). Thus, endogenously processed peptides were readily recognized by both receptors and activated T cell effector functions.

TCR-grafted T cells efficiently target HBV-infected cells in vitro

Our next step was to assess the antiviral capacity of TCR-grafted T cells on HepG2 cells stably expressing the HBV entry receptor NTCP (HepG2-NTCP) and infected with HBV. Based on titration experiments (Supplemental Figure 1A-F), we incubated the HBV-infected cells with TCR-grafted T cells at an effector to target (E:T) cell ratio of 1:2 and tested whether this would be sufficient to eliminate HBV-infected cells. After 6 and 10 days of co-culture, viral HBsAg and HBeAg were not detected anymore in cell culture media, respectively (Figure 2A,B), while secreted and intracellular viral rcDNA were largely reduced (Figure 2C,D). Most importantly, the persistence form of the viral DNA – cccDNA – became undetectable by qPCR after ten days (Figure 2E). A more prominent effect on cccDNA than on rcDNA was expected, since

rcDNA is protected from DNase activity within the HBV capsid (18). The amount of extracellular rcDNA even increased temporarily when infected cells were lysed by HBV-specific T cells (Figure 2C), likely because of the release of non-enveloped DNA-containing capsids (25).

To assess whether pre-treatment with antivirals would influence antiviral T cell activity, we treated HBV-infected cells with the NUC Entecavir (ETV) for three weeks before adding TCR-grafted T cells. While killing of ETV-treated target cells within 72 hours was reduced (Figure 2F), the overall antiviral effect of HBV-specific T cells remained equally pronounced compared to that without NUC treatment (Figure 2G-J). Thus, both core- and S-specific T cells generated by genetic engineering were capable of eliminating HBV-infected cells even after treatment with NUCs.

HBV-specific TCRs mediate redirection of T cells from patients with chronic hepatitis B

Adoptive T cell therapy imposes the challenge of creating an autologous T-cell product from a patient that has high viral antigens circulating and chronic inflammatory liver disease. Therefore, we used PBMC from two CHB patients, grafted T cells with the two selected TCRs and evaluated their antiviral potency. T cells could be transduced as efficiently as T cells from healthy donors (Figures 3A, 1A). T cell expansion was more than 200-fold, starting from less than a million cells, irrespective of the donor or the TCR being expressed (Figure 3B). $4G_{S20}$- and $6K_{C18}$-grafted T cells killed infected cells (Figure 3C) and secreted up to 10 ng/ml of IFN-γ within 2 days (Figure 3D). After 10 days of co-culture, secreted HBeAg became negative - with the exception of $4G_{S20}$ T cells in donor 2 where very low levels were still detected - and cccDNA was not detectable anymore (Figure 3E-F). Importantly, T cells from CHB patients did not inherently contain a relevant number of functional HBV-specific T cells before TCR-grafting, as no antiviral activity of mock-transduced T cells was observed.

Adoptive T cell therapy using T cell receptors entails that the TCR is customized to fit to the patient´s HLA-type. Therefore, we asked whether our high-affinity TCRs would recognize peptide presented on different HLA-A*02 subtypes (Supplemental Figure 2). In total, TCR $4G_{S20}$ or $6K_{C18}$ recognized their cognate peptide on 9/12 or 7/12 tested HLA-A*02-subtypes, respectively, including subtypes A*02:03, A*02:06 and A*02:07 which are most frequently found among the Asian population. Taken together, these TCRs conferred HBV-specificity to T cells from donors with CHB with a performance comparable to T cells from healthy donors and can be applied to patients with different HLA-A*02 subtypes.

TCR-grafted CD4$^+$ and CD8$^+$ T cells show antiviral activity

To quantify the contribution of $CD4^+$ T cells in controlling and eliminating HBV, infected cells were first co-cultured either with a mixture of $CD4^+$ and $CD8^+$ TCR-grafted T cells or with TCR-grafted $CD4^+$ T cells only. The combination of $CD4^+$ and $CD8^+$ T cells grafted with either TCR killed infected cells even at a starting E:T ratio as low as 1:64 (Figure 4A). $CD4^+$ T cells were also able to kill infected cells, although less efficiently requiring a 4-fold higher number of transduced T cells i.e. a higher E:T ratio (Figure 4B). Cytotoxic effector function of core-specific T cells started immediately after onset of the co-culture while that of S-specific T cells only started 1 or 2 days later. Secreted HBeAg declined 2-3 days after the onset of cytotoxicity (Supplemental Figure 3A,B). A direct comparison of both T cell types revealed that $CD8^+$ T cells mainly produced IFN-γ and $CD4^+$ T cells TNF-α in particular when using TCR $4G_{S20}$ (Figure 4C,D and Supplemental Figure 3C). Overall, $CD8^+$ T cells showed a stronger antiviral effect, and $CD4^+$ T cells that carried TCR $6K_{C18}$ were more efficient than $CD4^+$ T cells grafted with the TCR $4G_{S20}$ (Figure 4E,F and Supplemental Figure 3D,E). Taken together, not only $CD8^+$, but also $CD4^+$ T cells were able to kill HBV-infected cells when expressing a TCR with a high functional avidity.

174

175 ***TCR-grafted T cells clear HBV infected cells mainly by direct cytotoxicity***

176 Both cytotoxicity and secretion of cytokines by T cells play a role in viral clearance. To
177 determine the contribution of non-cytotoxic, cytokine-mediated antiviral activity of TCR-
178 grafted T cells, cytokine-depleting antibodies were employed in our in vitro infection model.
179 The antibodies reduced the amount of IFN-γ by about 60 and 90% for $4G_{S20}$- and $6K_{C18}$-
180 expressing T cells, respectively, and almost completely depleted TNF-α from the cell culture
181 medium (Figure 4C,D and Supplemental Figure 4A,B). Reduction of secreted HBeAg
182 remained similar when cytokines were deprived (Figure 4E, Supplemental Figure 4C). While
183 cccDNA levels remained strongly reduced when co-cultures with $CD8^+$ T cells were treated
184 with cytokine-blocking antibodies, cytokine removal reduced the capacity of $CD4^+$ T cells to
185 eliminate cccDNA (Figure 4F). A detailed comparison of $4G_{S20}$- and $6K_{C18}$-expressing T cells
186 showed that cccDNA clearance was reduced by a factor of 1.5-2 when IFN-γ and TNF-α were
187 neutralized (Figure 4G). This indicated that TCR-grafted $CD8^+$ T-cells mainly clear HBV by
188 direct cytotoxicity, while TCR-grafted $CD4^+$ T cells elicit both a cytotoxic and a prominent
189 non-cytotoxic, cytokine-mediated effect.

190 The high cytolytic T cell activity in vitro raised the concern of potential bystander killing of
191 non-infected cells. To address this concern, HBV-infected HepG2-NTCP cells MOI 100, about
192 half of the cells productively infected with HBV (26)) were mixed with non-infected cells at
193 different ratios. Interestingly, $4G_{S20}$-specific T cells were not activated when only 20% of cells
194 were derived from the infection cell batch while $6K_{C18}$ T cells still were (Supplementary Figure
195 5A-C). For both receptors, $4G_{S20}$ and $6K_{C18}$, killing increased directly proportionally to the
196 percentage of cells from the infected batch (Supplementary Figure 5A,B). When T cells were
197 activated for 24 hours by co-culture with HepG2-NTCP cells, which had been infected at MOI

of 500 and transferred to non-infected cell cultures, no bystander killing was observed while T cells remained active on infected cells (Supplementary Figure 5D). From these data we did not get any indication of non-specific activity of our TCR-grafted T cells.

Transfer of TCR grafted T cells results in strong reduction of HBV markers in vivo

For the clinical success of adoptive T cell therapy of CHB it is important that transferred T cells migrate to the liver, exert their effector function and eliminate HBV while liver function is maintained despite a loss of infected hepatocytes. In a first set of experiments we employed human liver chimeric USG mice harboring HLA-A*02-positive human hepatocytes to assess the antiviral activity of T cells stably expressing the selected HBV-specific TCRs. Mice were infected with HBV for 12 weeks and displayed median viral titers of $1.4x10^8$ (2.4×10^6 to $2.2x10^9$) HBV-DNA copies/ml before they received one single injection of either $2x10^6$ mock transduced or $1x10^6$ 6K- together with $1x10^6$ 4G-grafted T cells. They were followed-up either for a short time of 15-20 days or a longer time of 55 days (Figure 5A). Two additional mice (1 treated and 1 mock control) received a second injection of T cells at day 5 and were sacrificed at day 15. Alanine aminotransferase levels (ALT) were increased between day 3 and 7 post T-cell transfer in all mice that had received HBV-specific T cells indicating transient liver damage (Figure 5B). Liver damage was accompanied by a <10% transient body weight reduction (Supplementary Figure 6A). Mock-treated animals had ALT levels comparable to untreated liver chimeric mice indicating that no alloreaction was caused by the transferred T cells. In these high viremic, HBV-infected mice treated with TCR-grafted T cells, human serum albumin (HSA) decreased substantially (average 5.7-fold) (Figure 5C). Nevertheless, HSA levels started to slowly rebound in some animals (Figure 5C). Within the first 3 weeks after T-cell transfer, viremia decreased by $\approx 4\log_{10}$ (Figure 5D), and HBeAg and HBsAg dropped below the limit of detection in most animals (Figure 5E, F). At sacrifice, HBeAg proved non-reactive

in 6/7 and HBsAg in 3/7 mice treated with TCR-grafted T cells, and reduction of HBV DNA viremia was confirmed (Supplemental Figure 6B-D).

In line with the serological results, intrahepatic analyses of mice treated with effector T cells showed significantly lower levels (median: -3$\log_{10}$) of intracellular HBV RNA transcripts (Figure 5G) and rcDNA (Figure 5H) in comparison to mock-treated mice. In all treated mice intrahepatic cccDNA dropped to very low levels (median: - 2$\log_{10}$) 3 weeks after T cell transfer and became undetectable after 8 weeks of treatment (Figure 5I). The second T cell injection did not have any further effect, as one single injection of TCR-grafted T cell was already sufficient to achieve strong and sustained antiviral effects.

HBV pgRNA was not detectable by RNA in situ hybridization in liver tissues of mice that were sacrificed at day 18 (Figure 6A). The discrepancy between in situ and qPCR detection may be explained by the different sensitivity levels of the respective assays and by the fact that in situ analysis only reflects the viral state within a limited area of a liver section, since DNA and RNA for PCR analysis were extracted from a larger piece of liver tissue. Immunofluorescence co-staining for HBV core protein and human cytokeratin 18 (Figure 6B) revealed that nearly all human hepatocytes were HBV-positive in control mice with high viral titers, whereas animals with 10-fold lower viral titers (e.g. $2x10^8$ HBV-DNA copies/ml) had fewer positive cells (Figure 6B, mock-treated group). T-cell injection provoked a massive elimination of infected hepatocytes over time in mice with high infection rates (Figure 6B, upper panel), while in mice with intermediate infection rates at baseline, a large proportion of human hepatocytes survived (Figure 6B, lower panel). Human $CD45^+$ lymphocytes were still detected in liver tissue at day 19, but no longer after 8 weeks (Figure 6C). Nevertheless, human T cells, especially $CD8^+$ T cells, were still present in the spleen of mice 8 weeks post T-cell transfer, although the proportion of TCR^+ T cells had decreased compared to what had been injected in the mice (Supplemental Figure 7A, B). This could be attributed to downregulation of the TCR

after T cell activation or contraction of the population of HBV-specific T cells after most of the infection had been cleared. Of note, Ki67-staining showed the potential of human hepatocytes to proliferate and hence their ability to compensate for the immune-mediated cell loss (Figure 6D). Taken together, these experiments demonstrated that a single injection of T cells grafted with TCRs of high avidity can efficiently reduce HBV infection by promoting the clearance of HBV-infected hepatocytes in vivo.

TCR grafted T cells have the potential for clinical application

To assess the specificity with which effector T cells stably expressing HBV-specific TCRs target the infected hepatocytes in vivo without provoking damage of non-infected neighboring hepatocytes, we used mice in which only a minority of the human hepatocytes was infected. This mimics the clinical situation more closely, where typically only a low percentage of cells is infected and expresses HBV core and envelope proteins (27). To obtain partially HBV-infected humanized livers, we stopped HBV spreading at 5 weeks post virus inoculation by applying the HBV entry inhibitor MyrB. One week later, five mice received TCR-grafted T cells, whereas three animals served as controls and were sacrificed either 2 weeks (n=2) or 13 weeks after injection of mock T cells (Figure 7A). To assess whether HBV may relapse after T cell therapy, we stopped MyrB application in 2 mice 3 weeks after T cell transfer and monitored viremia levels for additional 10 weeks (i.e. until week 19 post infection).

In line with our previous experiments, a single injection of HBV-specific T cells caused a transient ALT elevation (Figure 7B) and concomitant reduction of HSA levels (Figure 7C) in all treated mice while their body weight remained stable (data not shown). Compared to high-titer HBV-infected mice (Figure 5C), HSA drop was less pronounced in the partially infected animals and HSA levels rebounded to baseline within 2-3 weeks (Figure 7C), indicating that

hepatocyte loss was limited and promptly compensated by human hepatocyte proliferation. HBV viremia, as well as circulating HBeAg and HBsAg dropped to borderline detection levels in all animals within two weeks after T cell transfer (Figure 7 D-F). When mice received MyrB throughout the experiment, intrahepatic levels of HBV transcripts and DNA were ≈4-log lower 3 and 13 weeks after transfer of TCR-grafted compared to mock T cells (Figure 7G-I). When MyrB treatment was stopped 3 weeks after T cell injection, all serological HBV markers started to rebound 9 weeks after injection of TCR-grafted T cells (Figure 7D-F) and reached baseline levels again at 13 weeks (Figure 7G-I). Co-staining of HBcAg and human CK18 revealed that only a minority of human hepatocytes was HBV-positive in mice that received MyrB at 5 weeks post infection and sacrificed 2 weeks post mock T-cell treatment (Figure 7J, left panel). HBV-positive cells were detected neither 3 nor 13 weeks after transfer of HBV-specific T cells under continuous MyrB treatment, whereas HBV-positive hepatocytes were detected in animals that discontinued MyrB treatment (Figure 7I, right panel). These results show that TCR-grafted T cells were able to target HBV-infected cells with high efficiency also when only a minority of human hepatocytes was infected. Lack of off-target effects also indicated high specificity of TCR-redirected T cells. Most importantly, HBV infection was fully controlled after adoptive transfer of HBV-specific T cells when MyrB was continuously administered.

Discussion

T cell therapy of CHB aims at supplementing a patient´s lacking or functionally exhausted HBV-specific T cell repertoire to achieve HBV control. In this study, we demonstrate that T cells genetically engineered to stably express HBV-specific TCRs with high functional avidity (21) are able to eliminate HBV-infected cells with high efficiency and specificity. Although our TCRs were cloned from European donors, testing them on different HLA-A2 subtypes showed a broad applicability irrespective of the patient's ethnicity. HBV-specific T cells obtained using either T cells of healthy volunteers or CHB patients expanded to clinically relevant numbers, were equally efficient and able to eliminate HBV-infected cells. Importantly, a single adoptive T cell transfer combined with administration of the HBV entry inhibitor MyrB was able to achieve long-term control of HBV infection in HBV-infected humanized mice.

Currently approved polymerase inhibitors are well tolerated and effectively suppress HBV replication. However, they do not directly affect the HBV persistence form, the cccDNA demanding additional means to cure hepatitis B (28). T cells grafted with HBV-specific receptors become activated by HBV-expressing hepatoma cell lines (20, 29) or HBV-infected hepatocytes (30) and target HBV persistence (18).

Our TCRs proved to be functional not only on $CD8^+$ but also on $CD4^+$ T cells, and grafting onto healthy volunteers' or CHB patients' T cells lead to elimination of viral antigens as well as cccDNA when co-cultured with HBV-infected cells. Both cell types showed cytotoxic and non-cytotoxic effector function while $CD8^+$ T cells mainly produced IFNγ and $CD4^+$ T cells TNFα. Thus, the manufacturing of a T cell product for clinical application can be simplified as purification of $CD8^+$ T cells will not be essential to generate sufficient numbers of antiviral T cells. As it has been shown that the inclusion of $CD4^+$ T cells grafted with a chimeric antigen receptor has a synergistic antitumor effect (31), $CD4^+$ T cells engrafted with our MHC-I-restricted high affinity TCRs that are fully functional without CD8 co-receptor binding (21)

315 will also very likely contribute to the success of adoptive T cell therapy either by direct antiviral
316 activity or by helper function.

317 Several cytokines, secreted by adoptively transferred T cells or after bystander activation of
318 other immune cells have been reported to influence HBV gene expression and replication in a
319 non-cytolytic fashion (32) by a number of different means (summarized in (33)). In our
320 experiments, however, killing of infected cells was the dominant antiviral mechanism
321 eliminating HBV in cell culture and in vivo. Since IFNγ, however, could only partially be
322 blocked by antibodies, the non-cytolytic effect of TCR-grafted T cells that has recently been
323 reported (29, 34) may have been underestimated in our experiments.

324 In our first in vivo experimental setting, most human hepatocytes (>90%) were infected with
325 HBV and mice were highly viremic after the virus had had 12 weeks to spread in the
326 immunodeficient animals. In these animals, a large proportion of the human cells was
327 eliminated upon T cell transfer, cccDNA was reduced by >95% and neither HBV core protein
328 nor viral RNAs could be detected anymore in situ in surviving human hepatocytes.
329 Nevertheless, non-cytolytic activity of T cells (29, 35) may have contributed to clear HBV
330 infection, since some human hepatocytes may well have lost cccDNA by cell division (11), as
331 demonstrated by positive Ki67 staining, and T-cell derived cytokines may have contributed to
332 purging (10, 29) or silencing (6) of cccDNA molecules.

333 A concern about HBV-specific T-cell therapy is the loss of a significant part of functional liver
334 cells, particularly in patients with liver cirrhosis and end-stage liver disease. After adoptive T
335 cell therapy, adverse events have been observed when the TCR was specific for a tumor-
336 associated (self-) antigen and bound "off-target" to related peptides (36), or when it recognized
337 the cognate antigen "off-organ" on healthy tissue (37). Both scenarios seem unlikely to happen
338 during T-cell therapy of CHB, as the viral antigens we are targeting are very distinct from "self-
339 antigens" and are only expressed in hepatocytes. This is supported by the notion that no severe

side effects have been noted after the transfer of HBV-specific immune cells to CHB patients with hematological malignancies and normal liver function, in whom bone marrow transplantation led to viral clearance while only causing moderate liver toxicity (14-16). In this regard, we found that despite the capacity of our engineered T cells to clear infected cells, cytotoxicity of the stably transduced T cells was limited, since ALT indicating hepatocyte death increased only transiently in the first week after T cell transfer. Serum HSA reflecting hepatocyte function dropped in correlation with the amount of intrahepatic infection detected. Humanized mice in which - as in a typical clinical setting - the liver was only partially infected neither lost weight nor showed any other signs of distress. Of note, TCR-grafted T-cells did not cause any measurable damage of neighboring non-infected cells, since large hepatocyte areas were maintained and HSA rebound to baseline levels emphasizing the capacity of human hepatocytes to proliferate and compensate for the immune-mediated cell loss.

The situation was different when virtually all human hepatocytes were infected. Here, we found a significant drop in HSA indicating a significant reduction in liver function. A fully infected liver, however, is not expected to reflect the situation of the majority of CHB patients (27). Another limitation of the humanized mouse model is the mismatch of human cytokines and murine receptors that may underestimate the effect of a cytokine storm. Huang et al. (38) showed in a study including more than one hundred HBeAg-negative patients, that in patients with a viral load below $1x10^6$ copies/ml the amount of $HBcAg^+$ hepatocytes is below 20%. Hence, patients, which would be considered as candidates for the clinical application of T cell therapy, should be carefully selected for their viremia and antigenemia. Nevertheless a liver biopsy should be obtained to assess the number of HBV-infected cells as well as the extend of pre-existing liver inflammation and fibrosis.

Treatment with NUCs only blocks the viral polymerase and production of new viral progeny, but not transcription of HBV RNA and antigen production per se. Thus, the presentation of

HBV antigen is not expected to change substantially and HBV-specific T cells should remain able to clear infected cells. Our in vitro study proved that recognition and clearance capacity of TCR-grafted T cells was maintained upon Entecavir treatment. Pretreatment with NUCs would even be preferred, since long term NUC treatment is associated with a lower extend of intrahepatic HBV infection (27). As in our experiments with partially infected mice, we would expect a less pronounced hepatocyte loss in patients that have received NUCs for some years and this should not impair liver function in non-cirrhotic or child A patients. Moreover, treatment with polymerase inhibitors will also reduce inflammation and thus increase safety of adoptive T-cell therapy. Safety could further be increased if a safeguard molecule would be co-transduced and co-expressed with the TCR to allow for rapid depletion of transferred T cells. To limit the circulation of HBV-specific T cells, the application of T cells that only transiently express the HBV-specific TCR after RNA electroporation is explored (22). However, in the same humanized mouse model TCR-electroporated T cells led to a comparable increases of ALT, but despite several T-cell re-injections did not achieve the same strong antiviral effect as their retrovirally transduced counterparts (22), and was even lower when resting, non-cytolytic T cells were used (34).

The efficacy of our retrovirally transduced T cells carrying high-avidity TCRs was striking in vivo, especially when compared to previous studies (22, 34). These results point out how a different technology used to engineer effector T cells (i.e. careful selection of TCRs (21) and stable versus transient TCR expression) helps to achieve a higher efficacy of T cell therapy. We needed only a single T cell injection to achieve a sustained drop of HBsAg and HBV DNA (> 4log) in the serum of mice, whereas multiple injections of transiently transduced T cells were needed to achieve a reduction of HBV viremia by a median 1 log, and HBsAg levels barely changed (22).

However, in the absence of adaptive immune responses, even the smallest HBV reservoir persisting eventually leads to viral rebound in our mice. To avoid HBV rebound, we combined T cell therapy with administration of the entry inhibitor MyrB and by this mean succeeded in maintaining control of HBV infection for the entire period of three months after T cell transfer. Although in CHB patients - in contrast to our immune incompetent mouse model – long term survival of transferred T cells is more likely and may even be supported by reconstitution of the patient´s own anti-HBV immune response, inhibition of new infection events will have a supportive role also in the clinical setting.

Adoptive T cell therapy of HBV-related diseases is already proceeding towards the clinics. Bertoletti and colleagues recently reported T cell therapy of an HLA-A2-positive patient who had received an HLA-A2-negative liver transplant because of HCC and developed metastases from his original HBV S^+, HLA-$A2^+$ HCC. This patient was treated with retrovirally TCR-grafted, S_{20}-specific T cells. The therapy was safe and circulating HBsAg decreased (17). Although these study results are very encouraging numbers of TCR-grafted, transferred HBV-specific T cells were low (<2.5% within $3.9x10^8$ infused cells). By improved retroviral transduction we can now generate high numbers of HBV-specific T cells stably expressing TCRs (>75% within $2.5x10^8$ cells) from less than one million cells from healthy donors but - as shown here - also from CHB patients even allowing to spare leukapheresis.

Taken together, we show that high-affinity HBV-specific T cells can be generated by TCR-grafting irrespective of the donor being HBV-positive or -negative prior to T cell therapy. TCR-grafted T cells have a strong antiviral capacity in cell culture and in vivo, most strongly reducing cccDNA, which is regarded as a hallmark of virological cure (3). Thus, adoptive T-cell therapy of CHB, mimicking T-cell responses in self-limiting HBV infection, may result in functional cure of HBV infection.

Materials and Methods

Retroviral transduction of T cells. Stable 293GP-R30 (RD114-pseudotype) producer cells were generated by transduction with cell culture supernatant from 293GP-GLV9 cells, both provided by BioVec Pharma (39) that had been transfected with TCR plasmids as described earlier (21). T cells were enriched using human T activator CD3/CD28 Dynabeads (Thermo Fisher Scientific, Waltham, MA, USA) and pre-stimulated for 2 days in T-cell medium (TCM): RPMI, 10 % human serum, 1 % pen/strep, 1 % glutamine, 1 % sodium pyruvate, 1 % non-essential amino acids, 0,01M HEPES (all Thermo Fisher Scientific), supplemented with 300 U/ml IL-2. 0.45 µm-filtered retrovirus cell culture supernatant from stable producer cell lines was centrifuged at 2000xg, 32°C for 2 hours on non-treated culture plates coated with 20 µg/ml RetroNectin (Takara, St. Germain en Laye, France). Retrovirus cell culture supernatant was removed and T cells were spinoculated onto the retrovirus-coated plate at 1000xg for 10 minutes. A second transduction was performed after 24 hours. TCR expression was determined by flow cytometry. Staining was done for 30 minutes on ice in the dark, using the primary antibodies anti-human CD4_APC (clone OKT4, #17-0048-42, eBioscience, Frankfurt, Germany), anti-human CD8_PB (clone DK25, #PB984, Dako, Waldbronn, Germany) and anti-mouse TCRβ_PE (clone H57-597, #553172, BD Biosciences, Heidelberg, Deutschland) diluted in FACS Buffer (0.1% BSA/PBS). Cells were analyzed using a FACSCanto II flow cytometer (BD Biosciences) and data were analyzed with FlowJo 9.2 software.

Co-culture with HBV-infected cells. HepG2 cells expressing the sodium-taurocholate cotransporting polypeptide (HepG2-NTCP K7, generated by our group (26)) were seeded in DMEM (10% FCS, 1% penicillin/streptomycin, 1% glutamine, 1% NEAA) on collagen-coated plates. At 90% confluency, 2.5% DMSO was added to the medium. Cells were infected 2-6 days later with HBV genotype ayw purified via heparin column affinity chromatography followed by sucrose gradient ultracentrifugation from HepAD38 cell culture supernatant in the

presence of 4.8% PEG overnight at the indicated number of virions per cell (MOI), and maintained with 1% FCS as a monolayer. For T-cell co-culture, medium was changed to DMEM 10% FCS / 2% DMSO. T cells were added in equal amounts of TCM (final concentration of 1% DMSO in co-culture) at the indicated ratio of $6K_{C18}$ (specific for C18-27: FLPSDFFPSV), or $4G_{S20}$ (specific for S20-28: FLLTRILTI) T cells to target cells (E:T). For Figure 2 F-J, HepG2-NTCP cells were infected with an MOI of 500. One week after infection cells were treated with 0.1 µM of Entecavir (ETV) twice a week for a duration of three weeks. For Figure 4 C-F, $CD8^+$ and $CD4^+$ T cells were separated using MACS beads for positive selection of the respective cell type (Miltenyi Biotech, Bergisch-Gladbach, Germany) and added at an E:T ratio of 1:2. Cytokine-blocking antibodies against IFN-γ (10ng/ml, clone B27, #506513, Biolegend, San Diego, CA, USA) or TNF-α (5ng/ml, clone D1B4, #7321, Cell Signaling, Danvers, MA, USA) were given every other day when medium was exchanged.

Analyses of co-cultures. Cytokines in the cell culture supernatant were detected using ELISA kits for IFN-γ and IL-2 (BioLegend, San Diego, USA) or for TNF-α (BD Biosciences). HBeAg in the cell culture supernatant was measured using the Enzygnost HBe monoclonal assay (Siemens Healthcare Diagnostics, Eschborn, Germany). Total DNA was extracted from cells using the NucleoSpin tissue kit (Macherey-Nagel, Düren, Germany) or from cell culture supernatant using a Tecan extraction robot (40). Viral DNA forms were amplified and detected by PCR as described previously (10) and quantified with a standard obtained from accredited assays in our diagnostics department. 7.5 µl DNA were digested with 5 units of T5 exonuclease (NEB, Ipswich, USA) for 30 minutes at 37°C to eliminate rcDNA before cccDNA quantification.

Real-time cytotoxicity measurement. $5x10^4$ HepG2 (ATCC®) or HepG2.2.15 cells (kind gift of Heinz Schaller, University of Heidelberg, Germany) prepared as described previously (21), or $4x10^4$ infected or non-infected HepG2-NTCP cells were seeded onto 96-well electronic

464 microtiter plates. T cells were added 1-2 days later when target cells had reached confluence.
465 The impedance, which reflects adherence of the target cells to the bottom of the plate, was
466 measured every 15-30 minutes using an xCELLigence® SP real-time cell analyzer (ACEA
467 Biosciences, San Diego).

468 ***Adoptive T cell transfer in humanized mice.*** Human liver chimeric mice were generated using
469 male or female, 3-week-old uPA/SCID/beige/IL-2Rγ-/- (USG) mice (41). They originated from
470 IL-2Rγ ko mice (JAX Mice stock number 003169; C.129S4-Il2rg<tmlWjl>/J) were backcrossed
471 10 times on uPA/SCID mice, which originated from crossing uPA mice (Jax Stock JR2214 (not
472 available anymore); B6SJL-TgN(Alb1Plau)144Bri) for 10 generations on SCID beige mice
473 (Taconic model: CBSCBG; C.B-Igh-1b/GbmsTac-Prkdcscid-Lystbg N7. After transplanting
474 $1x10^6$ thawed human HLA-$A2^+$ hepatocytes the repopulation levels were determined by
475 measuring human serum albumin (HSA) in mouse serum using the human Albumin ELISA
476 quantitation kit (Bethyl Laboratories, Biomol GmbH, Hamburg, Germany). To establish HBV
477 infection, animals received a single intra-peritoneal injection of HBV-infectious serum (1×10^7
478 HBV-DNA copies/mouse; genotype D) 10 weeks after transplantation. For adoptive T cell
479 transfer, T cells were thawed and cultured overnight in AIM-V medium (Gibco/Thermo Fisher
480 Scientific), 2% human AB^+-serum and 180 IU/ml rIL-2. $2x10^6$ TCR-grafted T cells ($1x10^6$ with
481 $6K_{C18}$ + $1x10^6$ with $4G_{S20}$) or equal numbers of mock-treated T cells were injected
482 intraperitoneally into HBV-infected mice. In the first experiment, mice were monitored until day
483 15-19 (short-term) or day 55 (long-term) after transfer. In the short-term follow-up groups, one
484 mouse of each group (both HBeAg 1.5 (S/CO) on day 3 post transfer) received a second injection
485 of $1x10^6$ TCR-grafted or mock T cells on day six (mice are specified in Figure 5) and one mouse
486 received MyrB, 5 days before sacrifice. In the second experiment, all mice received MyrB
487 (100µl; 2mg/kg) subcutaneously (11, 24) 5 weeks post infection to block the viral spreading and
488 mimic a partial infection in these mice. Within the first 5 days, mice received MyrB daily. After

5 days, mice were treated every other day to avoid re-or new-infection of non-infected hepatocytes. Blood was taken for analyses of viral antigens, ALT and viremia as indicated in results.

Virological measurements. DNA and RNA were extracted from liver specimens using the Master Pure DNA purification kit (Epicentre, Madison, USA) and RNeasy RNA purification kit (Qiagen), respectively. Intrahepatic total viral loads were quantified with the help of primers and probes specific for total HBV-DNA, pgRNA and cccDNA while the human housekeeping gene *GAPDH* was used for normalization (42). HBsAg and HBeAg quantification were performed on the Abbott Architect platform (Abbott, Ireland, Diagnostic Division) at indicated serum dilution. HBeAg results are displayed as signal to noise ratio (S/CO).

Analysis of biochemical parameters. ALT was measured by using the Roche Cobas c111 System (Roche, Basel, Switzerland). For the measurements 5µl of serum of the mice was used.

Preparation and staining of splenocytes. Spleens were dissected in cold mTCM (RPMI/10%FCS supplemented with Glutamin, 1% Pen/Strep, 0,1% beta-Mercaptoethanol and 1% sodium pyruvate, passed through a 100 µm strainer and homogenized through a 20 G needle. Splenocytes were centrifuged at 300xg for 5' at 4°C and incubated in TAC-buffer for 2' at 37°C to lyse erythrocytes. Reaction was stopped with mTCM. Cells were counted after repeat centrifugation and subsequently stained for anti-human CD8-PE-Cy7 (clone RPA-T8, #557746, BD Biosciences,), anti-human CD4-Pacific Blue (clone RPA-T4, #558116, BD Biosciences) and anti-mouse TRBC-PE (clone H57-597, #553172, BD Biosciences). Flow cytometry data were acquired on the BD FACS LSRII System.

Immunofluorescence and RNA in situ hybridization. Human hepatocytes were identified in frozen mouse liver sections using a monoclonal anti-human cytokeratin-18 mouse antibody (clone DC-10, #11-107-C100, Exbio, Praha, Czech Republic) or monoclonal anti-human calnexin rabbit antibody (clone C5C9, #2679, Cell Signaling Technology, Massachusetts, USA).

HBcAg staining was detected with anti-rabbit anti-HBcAg antibodies (polyclonal, #B0586, Dako Diagnostika, Glostrup, Denmark) and specific signals were visualized with Alexa 488- or Alexa 555-labelled secondary antibodies (polyclonal, #A21429, #A11029, # A11034, Invitrogen, Darmstadt, Germany) or the TSA Fluorescein System (Perkin Elmer, Jügesheim, Germany). Nuclear staining was achieved by Hoechst 33258 (Invitrogen, Eugene, USA). Human CD45 staining was performed using a monoclonal anti-mouse CD45 antibody (clone 2B11+PD7/26, # IS751, Dako). Proliferation of human hepatocytes and immune cells was determined using antibodies to human Ki-67 (polyclonal, # ABIN152984, antibodies-online, Aachen, Germany). RNA in situ hybridization was performed on paraformaldehyde-fixed, cryo-preserved liver sections using the RNAScope Fluorescent Multiplex Kit (Advanced Cell Diagnostics, ACD, Hayward, CA, USA) with target probes recognizing the pregenomic HBV (assay 442741-C2) and human beta2-microglobulin-RNA (assay 478171-C3). Stained sections were analysed by fluorescence microscopy (Biorevo BZ-9000, Keyence, Osaka, Japan) using the same settings for all groups.

Study approval. The use of healthy volunteer PBMC was approved by the local ethics board of the University Hospital rechts der Isar, Munich (G 548/15S), and written informed consent was obtained from all blood donors. PHH were isolated from rejected explant livers using protocols approved by the Ethical Committee of the city and state of Hamburg (OB-042/06) in accordance with the principles of the Declaration of Helsinki. Animals were housed under specific pathogen-free conditions according to institutional guidelines under authorized protocols. All animal experiments were approved by the City of Hamburg, Germany (G118/16), conducted in accordance with the European Communities Council Directive (86/EEC) and the ARRIVE standard.

Author contributions: K.W. and U.P. designed in vitro experiments. K.W., A.M. and T.A. performed in vitro experiments and K.W. analyzed data. K.W., J.K., M.D., and U.P. wrote the manuscript. T.B. provided and analyzed patient material. A.M. established transduction protocols. J.W. produced and purified HBV stocks. J.K., M.D., K.W and U.P. designed in vivo experiments. J.K. conducted in vivo experiments and acquired data. J.K. and K.W. analyzed the data. L.A. and T.V. generated human chimeric liver mice. M.L. and L.A. established RNA in situ hybridization assays. L.A. and J.K. performed RNA in situ hybridization assay. S.U. conceptually contributed to entry inhibition experiments and provided MyrB for the in vivo experiments. All authors discussed data and corrected the manuscript.

Acknowledgments:

This work was supported by the German Research Foundation (DFG) via TRR36 and TRR179 to U.P., SFB841 and a Heisenberg Professorship to M.D. (DA1063/3-2). U.P., M.D. and S.U. received funding from the German Center for Infection Research (DZIF, TTU Hepatitis 05.806, 05.704). K.W. received a Maternity Leave stipend and a young investigator grant from DZIF (TTU Hepatitis 05.812). We thank Ke Zhang for generating and Daniela Stadler for cloning HepG2NTCP cells, Wolfgang Uckert for providing optimized MP71 constructs and Michael Ostertag for creating retrovirus producer cell lines.

References

1. WHO. Global Hepatitis Report 2017. *Geneva: World Health Organization*. 2017:Licence: CC BY-NC-SA 3.0.

2. Trepo C, Chan HL, and Lok A. Hepatitis B virus infection. *Lancet*. 2014;384(9959):2053-63.

3. Lok AS, Zoulim F, Dusheiko G, and Ghany MG. Hepatitis B cure: From discovery to regulatory approval. *J Hepatol*. 2017;67(4):847-61.

4. Thimme R, Wieland S, Steiger C, Ghrayeb J, Reimann KA, Purcell RH, et al. CD8(+) T cells mediate viral clearance and disease pathogenesis during acute hepatitis B virus infection. *J Virol*. 2003;77(1):68-76.

5. Rehermann B, and Nascimbeni M. Immunology of hepatitis B virus and hepatitis C virus infection. *Nat Rev Immunol*. 2005;5(3):215-29.

6. Belloni L, Allweiss L, Guerrieri F, Pediconi N, Volz T, Pollicino T, et al. IFN-alpha inhibits HBV transcription and replication in cell culture and in humanized mice by targeting the epigenetic regulation of the nuclear cccDNA minichromosome. *J Clin Invest*. 2012;122(2):529-37.

7. Liu F, Campagna M, Qi Y, Zhao X, Guo F, Xu C, et al. Alpha-interferon suppresses hepadnavirus transcription by altering epigenetic modification of cccDNA minichromosomes. *PLoS Pathog*. 2013;9(9):e1003613.

8. Tropberger P, Mercier A, Robinson M, Zhong W, Ganem DE, and Holdorf M. Mapping of histone modifications in episomal HBV cccDNA uncovers an unusual chromatin organization amenable to epigenetic manipulation. *Proc Natl Acad Sci U S A*. 2015;112(42):E5715-24.

9. Guidotti LG, Rochford R, Chung J, Shapiro M, Purcell R, and Chisari FV. Viral clearance without destruction of infected cells during acute HBV infection. *Science*. 1999;284(5415):825-9.

582 10. Lucifora J, Xia Y, Reisinger F, Zhang K, Stadler D, Cheng X, et al. Specific and
583 nonhepatotoxic degradation of nuclear hepatitis B virus cccDNA. *Science*.
584 2014;343(6176):1221-8.

585 11. Allweiss L, Volz T, Giersch K, Kah J, Raffa G, Petersen J, et al. Proliferation of primary
586 human hepatocytes and prevention of hepatitis B virus reinfection efficiently deplete
587 nuclear cccDNA in vivo. *Gut*. 2018;67(3):542-52.

588 12. Bertoletti A, and Ferrari C. Innate and adaptive immune responses in chronic hepatitis B
589 virus infections: towards restoration of immune control of viral infection. *Gut*.
590 2012;61(12):1754-64.

591 13. Bohne F, and Protzer U. Adoptive T-cell therapy as a therapeutic option for chronic
592 hepatitis B. *J Viral Hepat*. 2007;14 Suppl 1:45-50.

593 14. Ilan Y, Nagler A, Zeira E, Adler R, Slavin S, and Shouval D. Maintenance of immune
594 memory to the hepatitis B envelope protein following adoptive transfer of immunity in
595 bone marrow transplant recipients. *Bone Marrow Transplant*. 2000;26(6):633-8.

596 15. Ilan Y, Nagler A, Adler R, Naparstek E, Or R, Slavin S, et al. Adoptive transfer of
597 immunity to hepatitis B virus after T cell-depleted allogeneic bone marrow transplantation.
598 *Hepatology*. 1993;18(2):246-52.

599 16. Lau GK, Lok AS, Liang RH, Lai CL, Chiu EK, Lau YL, et al. Clearance of hepatitis B
600 surface antigen after bone marrow transplantation: role of adoptive immunity transfer.
601 *Hepatology*. 1997;25(6):1497-501.

602 17. Qasim W, Brunetto M, Gehring AJ, Xue SA, Schurich A, Khakpoor A, et al.
603 Immunotherapy of HCC metastases with autologous T cell receptor redirected T cells,
604 targeting HBsAg in a liver transplant patient. *J Hepatol*. 2015;62(2):486-91.

605 18. Bohne F, Chmielewski M, Ebert G, Wiegmann K, Kurschner T, Schulze A, et al. T cells
606 redirected against hepatitis B virus surface proteins eliminate infected hepatocytes.
607 *Gastroenterology*. 2008;134(1):239-47.

608 19. Krebs K, Bottinger N, Huang LR, Chmielewski M, Arzberger S, Gasteiger G, et al. T cells
609 expressing a chimeric antigen receptor that binds hepatitis B virus envelope proteins
610 control virus replication in mice. *Gastroenterology*. 2013;145(2):456-65.

611 20. Gehring AJ, Xue SA, Ho ZZ, Teoh D, Ruedl C, Chia A, et al. Engineering virus-specific
612 T cells that target HBV infected hepatocytes and hepatocellular carcinoma cell lines. *J*
613 *Hepatol*. 2011;55(1):103-10.

614 21. Wisskirchen K, Metzger K, Schreiber S, Asen T, Weigand L, Dargel C, et al. Isolation and
615 functional characterization of hepatitis B virus-specific T-cell receptors as new tools for
616 experimental and clinical use. *PLoS One*. 2017;12(8):e0182936.

617 22. Kah J, Koh S, Volz T, Ceccarello E, Allweiss L, Lutgehetmann M, et al. Lymphocytes
618 transiently expressing virus-specific T cell receptors reduce hepatitis B virus infection. *J*
619 *Clin Invest*. 2017;127(8):3177-88.

620 23. Volz T, Allweiss L, Ben MM, Warlich M, Lohse AW, Pollok JM, et al. The entry inhibitor
621 Myrcludex-B efficiently blocks intrahepatic virus spreading in humanized mice previously
622 infected with hepatitis B virus. *J Hepatol*. 2013;58(5):861-7.

623 24. Petersen J, Dandri M, Mier W, Lutgehetmann M, Volz T, von Weizsacker F, et al.
624 Prevention of hepatitis B virus infection in vivo by entry inhibitors derived from the large
625 envelope protein. *Nat Biotechnol*. 2008;26(3):335-41.

626 25. Arzberger S, Hosel M, and Protzer U. Apoptosis of hepatitis B virus-infected hepatocytes
627 prevents release of infectious virus. *J Virol*. 2010;84(22):11994-2001.

628 26. Ko C, Chakraborty A, Chou WM, Hasreiter J, Wettengel JM, Stadler D, et al. Hepatitis B
629 virus genome recycling and de novo secondary infection events maintain stable cccDNA
630 levels. *J Hepatol*. 2018;69(6):1231-41.

631 27. Wursthorn K, Lutgehetmann M, Dandri M, Volz T, Buggisch P, Zollner B, et al.
632 Peginterferon alpha-2b plus adefovir induce strong cccDNA decline and HBsAg reduction
633 in patients with chronic hepatitis B. *Hepatology*. 2006;44(3):675-84.

634 28. Gehring AJ, and Protzer U. Targeting Innate and Adaptive Immune Responses to Cure
635 Chronic HBV Infection. *Gastroenterology*. 2019;156(2):325-37.

636 29. Xia Y, Stadler D, Lucifora J, Reisinger F, Webb D, Hosel M, et al. Interferon-gamma and
637 Tumor Necrosis Factor-alpha Produced by T Cells Reduce the HBV Persistence Form,
638 cccDNA, Without Cytolysis. *Gastroenterology*. 2016;150(1):194-205.

639 30. Hoh A, Heeg M, Ni Y, Schuch A, Binder B, Hennecke N, et al. Hepatitis B Virus-Infected
640 HepG2hNTCP Cells Serve as a Novel Immunological Tool To Analyze the Antiviral
641 Efficacy of CD8+ T Cells In Vitro. *J Virol*. 2015;89(14):7433-8.

642 31. Sommermeyer D, Hudecek M, Kosasih PL, Gogishvili T, Maloney DG, Turtle CJ, et al.
643 Chimeric antigen receptor-modified T cells derived from defined CD8+ and CD4+ subsets
644 confer superior antitumor reactivity in vivo. *Leukemia*. 2016;30(2):492-500.

645 32. Guidotti LG, and Chisari FV. Noncytolytic control of viral infections by the innate and
646 adaptive immune response. *Annu Rev Immunol*. 2001;19:65-91.

647 33. Xia Y, and Protzer U. Control of Hepatitis B Virus by Cytokines. *Viruses*. 2017;9(1).

648 34. Koh S, Kah J, Tham CYL, Yang N, Ceccarello E, Chia A, et al. Nonlytic Lymphocytes
649 Engineered to Express Virus-Specific T-Cell Receptors Limit HBV Infection by
650 Activating APOBEC3. *Gastroenterology*. 2018.

651 35. Guidotti LG, Ando K, Hobbs MV, Ishikawa T, Runkel L, Schreiber RD, et al. Cytotoxic
652 T lymphocytes inhibit hepatitis B virus gene expression by a noncytolytic mechanism in
653 transgenic mice. *Proc Natl Acad Sci U S A*. 1994;91(9):3764-8.

654 36. Morgan RA, Chinnasamy N, Abate-Daga D, Gros A, Robbins PF, Zheng Z, et al. Cancer
655 regression and neurological toxicity following anti-MAGE-A3 TCR gene therapy. *J*
656 *Immunother*. 2013;36(2):133-51.

657 37. Johnson LA, Morgan RA, Dudley ME, Cassard L, Yang JC, Hughes MS, et al. Gene
658 therapy with human and mouse T-cell receptors mediates cancer regression and targets
659 normal tissues expressing cognate antigen. *Blood*. 2009;114(3):535-46.

660 38. Huang YH, Hung HH, Chan CC, Lai CR, Chu CJ, Huo TI, et al. Core antigen expression
661 is associated with hepatic necroinflammation in e antigen-negative chronic hepatitis B
662 patients with low DNA loads. *Clin Vaccine Immunol*. 2010;17(6):1048-53.

663 39. Ghani K, Wang X, de Campos-Lima PO, Olszewska M, Kamen A, Riviere I, et al. Efficient
664 human hematopoietic cell transduction using RD114- and GALV-pseudotyped retroviral
665 vectors produced in suspension and serum-free media. *Hum Gene Ther*. 2009;20(9):966-
666 74.

667 40. Zhang K BC, Neumann-Fraune M, Xia Y, Beggel B, Kaiser R, Schildgen V, Krämer A,
668 Schildgen O and Protzer U. Novel rtM204 Mutations in HBV Polymerase Confer Reduced
669 Susceptibility to Adefovir and Tenofovir. *J Antivir Antiretrovir*. 2017;8:10-7.

670 41. Allweiss L, Volz T, Lutgehetmann M, Giersch K, Bornscheuer T, Lohse AW, et al.
671 Immune cell responses are not required to induce substantial hepatitis B virus antigen
672 decline during pegylated interferon-alpha administration. *J Hepatol*. 2014;60(3):500-7.

673 42. Giersch K, Allweiss L, Volz T, Helbig M, Bierwolf J, Lohse AW, et al. Hepatitis Delta
674 co-infection in humanized mice leads to pronounced induction of innate immune responses
675 in comparison to HBV mono-infection. *J Hepatol*. 2015;63(2):346-53.
676

677

Figures and Figure Legends

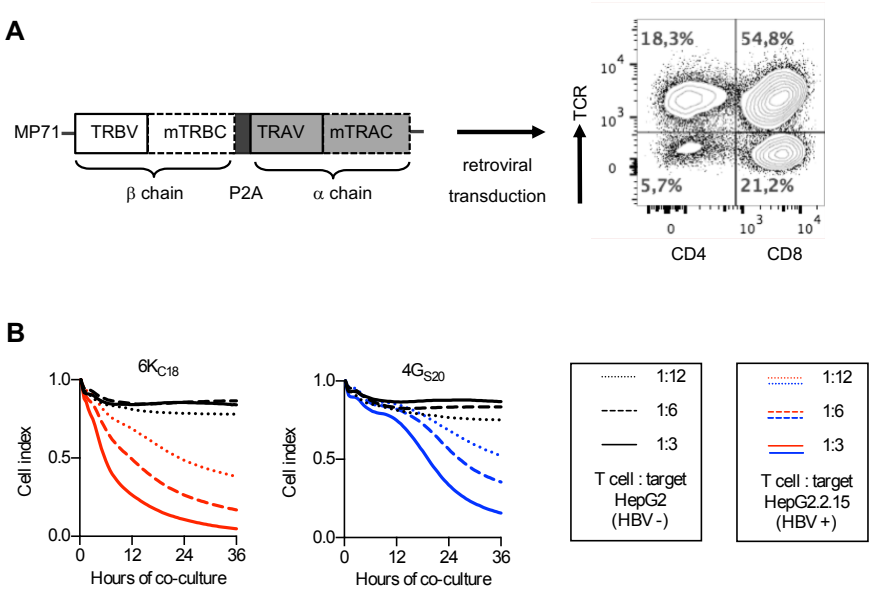

Figure 1. Genetic engineering and analysis of HBV-specific T cells. (**A**) Codon-optimized TCR α (TRAV) and β (TRBV) chains of high-affinity TCRs were cloned into the retroviral vector MP71. Murine constant domains (mTRBC, mTRAC) and insertion of additional cysteines were used to increase pairing. After retroviral transduction T cells were stained for mTRBC and TCR expression was quantified by flow cytometry. (**B**) Functional comparison scored eleven TCRs directed against HBV peptides $Core_{18\text{-}27}$, $S_{20\text{-}28}$ and $S_{172\text{-}180}$ (21). TCRs $6K_{C18}$ and $4G_{S20}$ were identified to have the highest functional avidity and were therefore chosen for further analyses: Parental HepG2 or HBV+ HepG2.2.15 target cells were co-cultured with increasing numbers of TCR-grafted T cells. Killing of target cells was determined by detachment from the plate using a real-time cell analyzer (XCelligence^{TM}) and is given as normalized cell index relative to the starting point of the co-culture. HBV^{-} target cells co-cultured with TCR-grafted T cells are shown as black lines. HBV^{+} target cells co-cultured with $6K_{C18}$ –transduced T cells are shown in red and $4G_{S20}$-transduced T cells in blue. Data are presented as mean values of quadruplicate co-cultures (n=4).

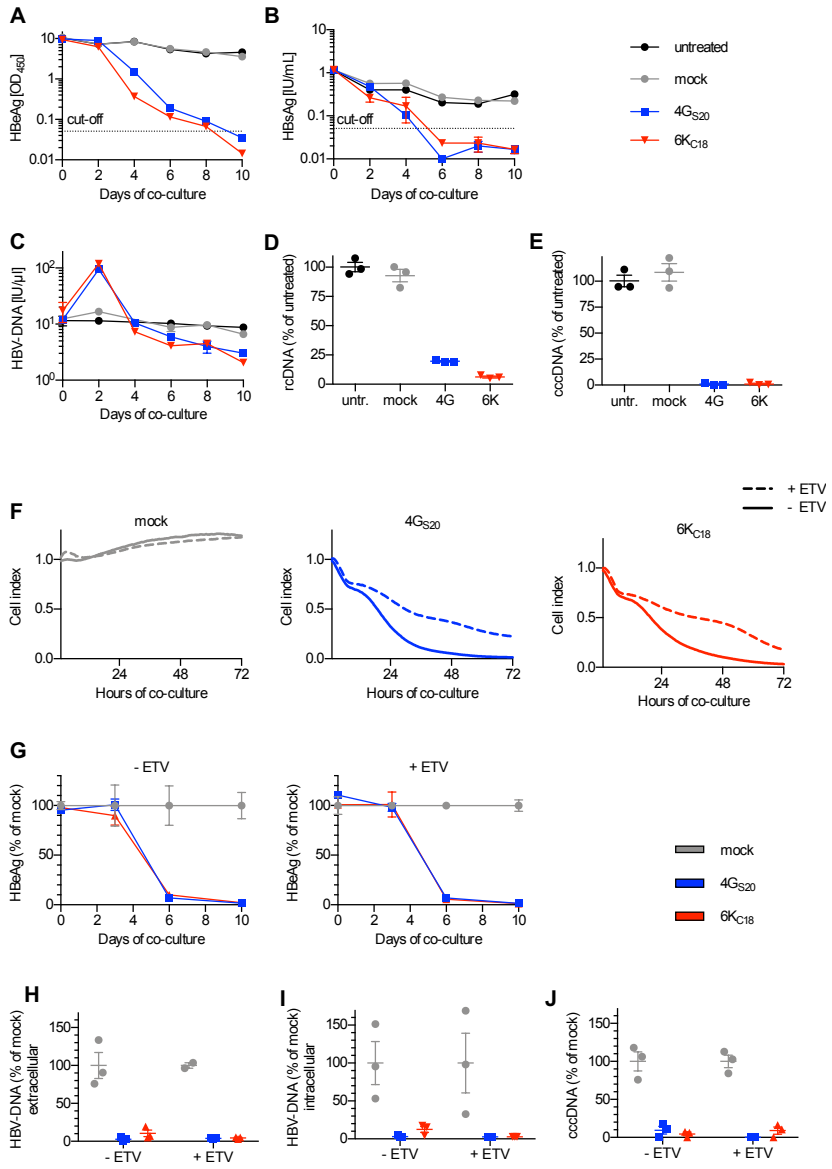

Figure 2. Antiviral effect of TCR-grafted T cells on HBV-infected cells. HepG2-NTCP cells were infected with HBV at an MOI of 100. After two weeks, T cells grafted with HBV S-specific TCR 4G$_{S20}$ (blue squares) or HBV core-specific TCR 6K$_{C18}$ (red triangles) or non-transduced T cells (mock, grey circles) were added for ten days at an E:T ratio of 1:2. Medium was changed every other day and used to determine (**A**) HBeAg and (**B**) HBsAg, by diagnostic ELISA. (**C**) HBV relaxed circular (rc)DNA contained in virions that had been secreted was extracted from cell culture supernatant every other day and DNA extracted from cell lysates on day ten was used to determine (**D**) intracellular HBV rcDNA and (**E**) nuclear cccDNA using qPCR. (**F-J**) Cells were infected with an MOI of 500. One week after infection cells were treated with 0.1 µM of Entecavir (ETV) twice a week for a duration of three weeks. (**F**) Killing of target cells was measured using a real-time cell analyzer and is given as normalized cell index relative to the starting point of the co-culture. E:T 1:1. (**G-J**) Medium was changed every 3-4 days and values are normalized for co-cultures treated with mock T cells. (**G**) HBeAg in supernatant of co-cultures without (left) or with (right) ETV pre-treatment (**H, I**) HBV relaxed circular (rc)DNA contained in virions secreted into the cell culture medium or extracted from cell lysates on day ten and (**J**) nuclear cccDNA determined using qPCR. Data are presented as mean values from triplicate co-cultures (n=3).

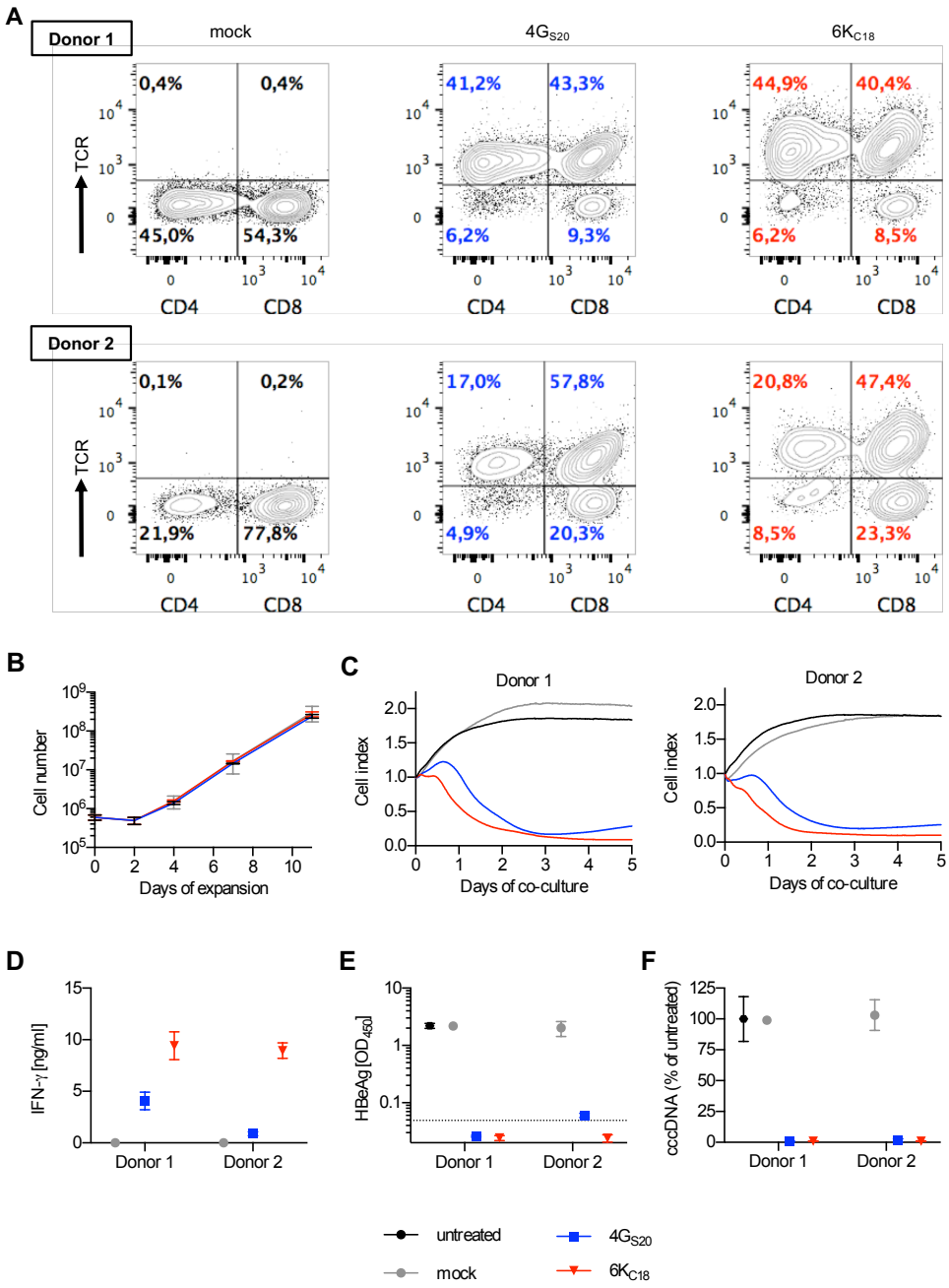

Figure 3. Antiviral activity of T cells from patients with CHB. (**A**) CD3$^+$ T cells were isolated from two donors with CHB and transduced to express HBV-specific TCRs 4G$_{S20}$ (blue) and 6K$_{C18}$ (red). TCR expression was quantified by flow cytometry. (**B**) Expansion of T cells during retroviral transduction with CD3/CD28 T activator Dynabeads and IL-2. (**C-F**) HepG2-NTCP cells were infected with HBV at an MOI of 500 three weeks prior to co-culture with TCR-grafted T cells from CHB donors at an E:T ratio of 1:2. Since the ratio of CD4$^+$ and CD8$^+$ T cells varied strongly between the donors, effector cell number was calculated on the basis of TCR$^+$ CD8$^+$ T cells only. (**C**) Killing of target cells was measured using a real-time cell analyzer and is given as normalized cell index relative to the starting point of the co-culture. E:T 1:2.7. (**D**) IFN-γ was determined in cell culture medium on day 2. Secreted HBeAg (**E**) and intracellular HBV cccDNA (**F**) were measured after 10 days of co-culture. Data are presented as mean values of triplicate co-cultures (n=3).

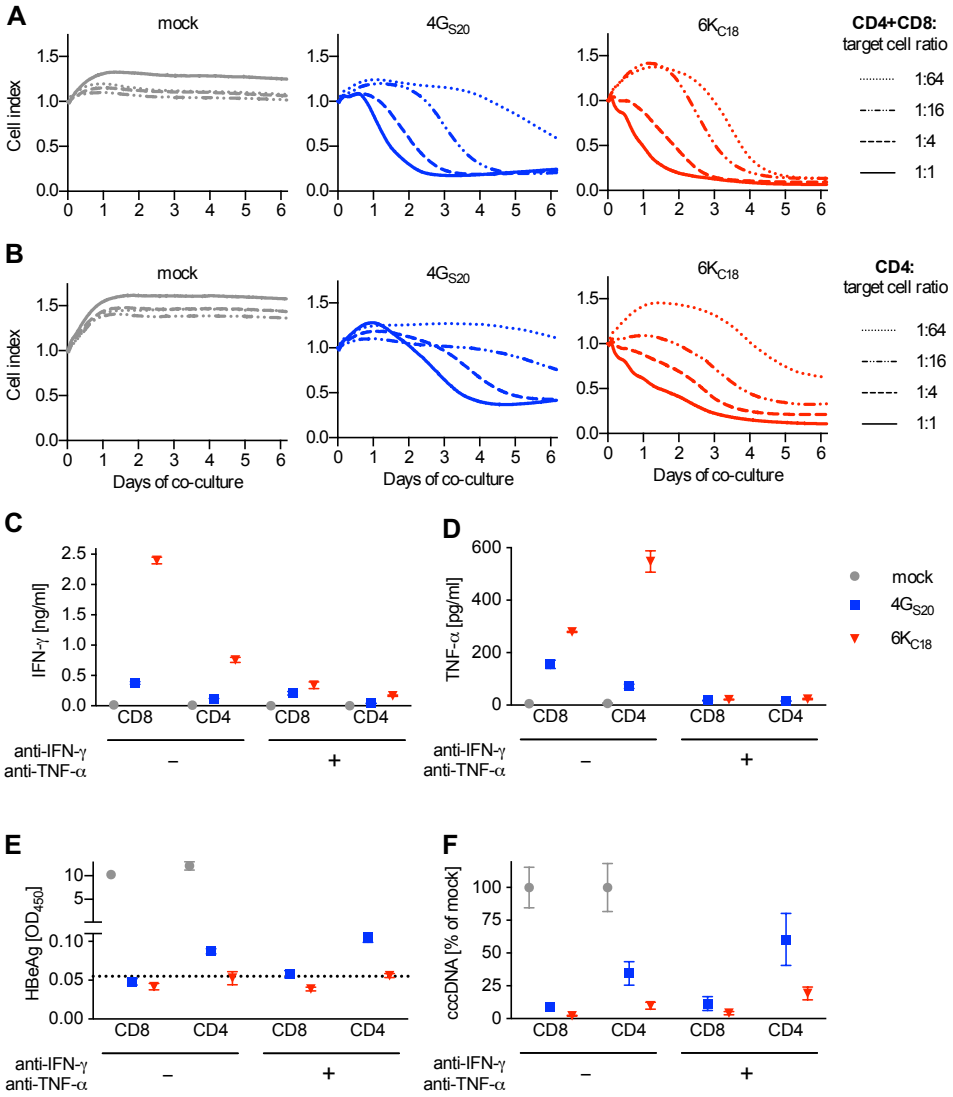

Figure 4. Antiviral activity of different TCR-grafted T cell subsets. HepG2-NTCP cells were infected with HBV at an MOI of 500. After two-three weeks, T cells grafted with TCR 4G$_{S20}$ (blue squares) or 6K$_{C18}$ (red triangles) or non-transduced T cells (mock, grey circles) were added at decreasing E:T ratios. (**A,B**) Killing of target cells determined by detachment from the bottom of the 96-well plate was measured in real-time (XCelligence™) and is given as normalized cell index relative to the starting point of the co-culture with CD4$^+$ and CD8$^+$ T cells (**A**) or CD4$^+$ T cells only (**B**). (**C-F**) CD8$^+$ and CD4$^+$ T cells were separated by positive magnetic cell sorting and added at an E:T ratio of 1:2. Cytokine-blocking antibodies against IFN-γ (10ng/ml) or TNF-α (5ng/ml) were given every other day when medium was exchanged. (**C, D**) IFN-γ and TNF-α were measured in the cell culture medium after 2 days. (**E**) Secreted HBeAg and (**F**) intracellular HBV cccDNA were measured after 10 days of co-culture. Data are presented as mean values (A,B) or mean values ± SEM (C-F) of triplicate co-cultures (n=3).

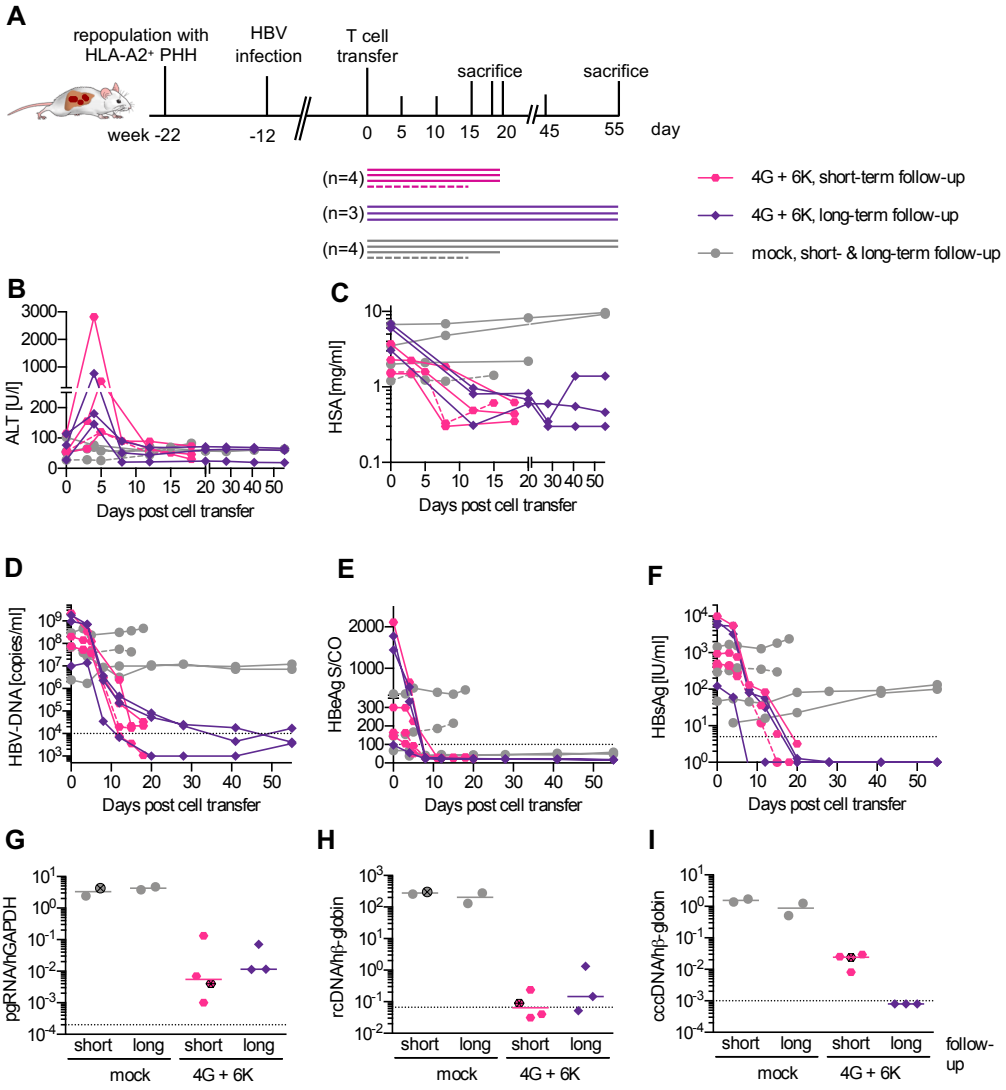

Figure 5. Antiviral activity of TCR-grafted T cells in HBV-infected humanized mice. (**A**) USG mice were repopulated with HLA-A*02-matched PHH, infected with $1x10^7$ HBV virions, followed until a stable viremia had established (week 12-14) and injected with $2x10^6$ TCR-grafted T cells ($1x10^6$ with $6K_{C18}$ plus $1x10^6$ with $4G_{S20}$; colored symbols, n=7) or equal numbers of mock-treated human T cells (grey circles, n=4). 4 mice were sacrificed within 3 weeks (short-term follow-up, pink hexagons) and 3 mice 8 weeks (long-term follow-up, purple diamonds) after T cell transfer, respectively. 2/11 mice received a second dosage of either effector cells or mock cells and were sacrificed on day 15 (presented by broken lines in A-F and crossed dots in G-I). (**B**) ALT activity and progression of (**C**) HSA or (**D**) HBV-DNA in sera. (**E, F**) HBeAg and HBsAg determined using immunoassays. **(G-I)** Intrahepatic HBV RNA and DNA transcripts were quantified by qPCR. (**G**) Levels of pregenomic HBV RNA were normalized to human GAPDH RNA. (**H, I**) rcDNA and cccDNA were quantified relative to an HBV plasmid standard curve and normalized to human beta globin. Each data point or longitudinal line represents one mouse. Dotted line represents the technical cut-off of the respective test. For DNA and RNA analyses dotted lines indicate the lower limit of detection = LLoD (defined as 10 HBV rcDNA or cccDNA copies per ≥1000 human beta globin copies).

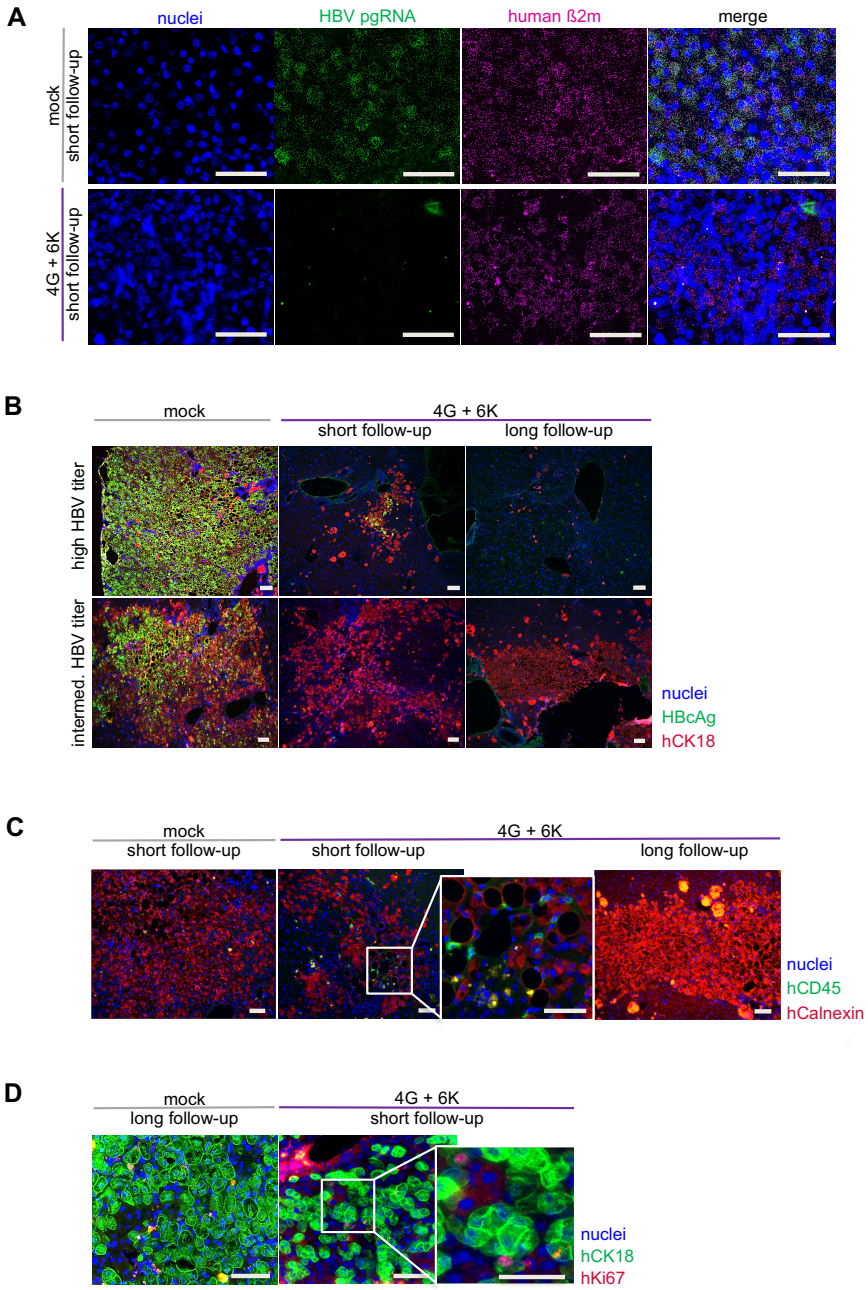

Figure 6. In situ analysis of antiviral effects of TCR-grafted T cells in humanized livers. Liver tissue of HBV-infected mice treated with mock-transduced T cells or $2x10^6$ HBV-specific T cells ($1x10^6$ with $6K_{C18}$ plus $1x10^6$ with $4G_{S20}$) were used from day 18-19 (short follow-up) or days 55 post T cell transfer (long follow-up). (**A**) In situ RNA hybridization for HBV pregenomic RNA (green) and human β2-microglobulin (magenta) against nuclei staining (blue) was performed to determine the occurrence of HBV specific RNA transcripts. (**B**) As indicated mice were distinguish in the level of infection into high (10^9-10^{10} copies/ml) or low (10^7-10^8 copies/ml) HBV titer. Representative immunohistochemistry staining for cell nuclei (blue), HBV core protein (green), and human cytokeratin 18 (red). (**C**) Human CD45 positive cells (green) were stained against human Calnexin (red) as marker for human hepatocytes and cell nuclei (blue). (**D**) To determine potential proliferation in mice treated with T cells, staining for cell nuclei (blue), human cytokeratin 18 (green) and Ki67 (red) was employed. Scale bar of liver tissue sections: 50µm.

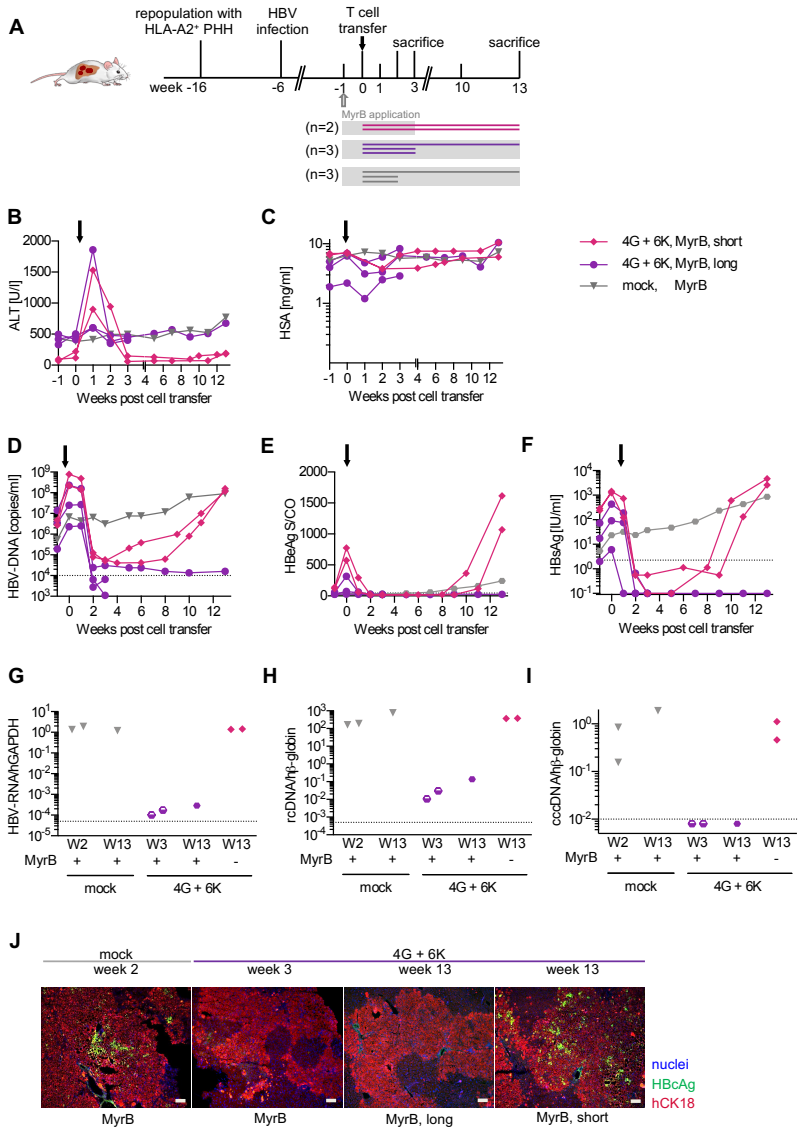

Figure 7. Long-term follow-up of mice partially infected with HBV and treated with HBV-specific T cells and an entry inhibitor. (**A**) USG mice were repopulated with HLA-A*02-matched PHH, infected with 1x10^7 HBV virions. Viral spreading was stopped at week 5 after infection by administration of MyrB (see methods) (grey blocks). After 1 week of MyrB application, 2x10^6 TCR-grafted T cells (1x10^6 with 6K$_{C18}$ plus 1x10^6 with 4G$_{S20}$, n=5) or mock T cells (grey triangles, n=3) were transferred. To address the question whether mice could be re-infected after treatment with effector T cells, MyrB application was stopped in 2/5 mice after 3 weeks (MyrB short, pink diamonds, n=2) and followed up till week 13. MyrB was administered continuously in 3/5 mice (MyrB long, purple hexagons, n=3). Mice were sacrificed at week 2 or 3 during short-term follow-up or at week 13 during long-term follow-up. Time course of ALT activity (**B**), HSA (**C**)**,** HBV viremia (**D**) HBeAg (**E**) and HBsAg (**F**) in sera followed until week 3 or 13, respectively. (**G**) Levels of pregenomic RNA were normalized to human GAPDH RNA. (**H, I**) rcDNA and cccDNA were quantified relative to an HBV plasmid standard curve and normalized to human beta globin. Each data point or longitudinal line represents one mouse. Dotted lines represent the technical cut-off of the respective test. For DNA and RNA analyses dotted lines indicate the lower limit of detection = LLoD (defined as 10 HBV DNA or cccDNA copies per ≥1000 human beta globin copies). Dots below LLoD symbolize undetectable measurements. (**J**) Representative staining of liver tissue slides from mice either treated with mock or 4G+6K effector T cells.